American Mineralogist, Volume 98, pages 1302–1309, 2013

Rapidcreekite in the sulfuric acid weathering environment of Diana Cave, Romania

Bogdan P. Onac,[1,2,*] Herta S. Effenberger,[3] Jonathan G. Wynn,[1] and Ioan Povară[4]

[1]Department of Geology, University of South Florida, 4202 E. Fowler Avenue, SCA 528, Tampa, Florida 33620, U.S.A.
[2]Emil Racoviţă Institute of Speleology/Department of Geology, Babeş-Bolyai University, Kogălniceanu 1, 400084, Cluj-Napoca, Romania
[3]Institut für Mineralogie und Kristallographie, Universität Wien, Althanstrasse 14, A-1090 Wien, Austria
[4]Emil Racoviţă Institute of Speleology, Frumoasă 31, 010986 Bucharest, Romania

Abstract

The Diana Cave in SW Romania develops along a fault line and hosts a spring of hot (T_{avg} = 51 °C), sulfate-rich, sodium-calcium-chloride bearing water of near-neutral pH. Abundant steam and H_2S rises from the thermal water to condensate on the walls and ceiling of the cave. The sulfuric acid produced by H_2S oxidation/hydrolysis causes a strong acid-sulfate weathering of the cave bedrock generating a sulfate-dominated mineral assemblage that includes rapidcreekite, $Ca_2(SO_4)(CO_3)\cdot 4H_2O$ closely associated with gypsum and halotrichite group minerals. Rapidcreekite forms bundles of colorless tabular orthorhombic crystals elongated along [001] and reaching up to 1.5 mm in length. For verifying the hydrogen bond scheme and obtaining crystal-chemical details of the carbonate group a single-crystal structure refinement of rapidcreekite was performed. Its unit-cell parameters are: a = 15.524(2), b = 19.218(3), c = 6.161(1) Å; V = 1838.1(5) Å^3, Z = 8, space group *Pcnb*. Chemical composition (wt%): CaO 35.65, SO_3 24.97, CO_2 13.7, H_2O 23.9, Na_2O 0.291, MgO 0.173, Al_2O_3 0.07, total 98.75%. The empirical formula, based on 7 non-water O atoms pfu, is: $Ca_{1.98}Na_{0.029}Mg_{0.013}Al_{0.004}(S_{0.971}O_4)(C_{0.97}O_3)\cdot 4.13H_2O$. The $\delta^{34}S$ and $\delta^{18}O$ values of rapidcreekite and other cave sulfates range from 18 to 19.5‰ CDT and from –9.7 to 7.8‰ SMOW, respectively, indicating that the source of sulfur is a marine evaporite and that during hydration of the minerals it has been an abundant ^{18}O exchange with percolating water but almost no oxygen is derived from $O_{2(aq)}$. This is the first description of rapidcreekite from a cave environment and one of the very few natural occurrences worldwide. We also report on the mineral stability and solubility, parameters considered critical to understand the co-precipitation of carbonates and sulfates, a process that has wide applications in cement industry and scaling prevention.

Keywords: Rapidcreekite, acid-sulfate weathering, hydrogen bond scheme, carbonate group, $\delta^{34}S$-$\delta^{18}O$ values, Diana Cave, Romania

Introduction

Sulfates are the largest group among cave minerals, with 89 species forming in a variety of settings (Hill and Forti 1997; Onac and Forti 2011a, 2011b). Of these, only gypsum, epsomite, and mirabilite may be considered common for cave environments, with gypsum perhaps the second most frequent cave mineral after calcite (Onac 2012). The majority of the other sulfates only occur under very particular settings, such as in caves located nearby ore deposits or thermo-mineral water sources and in areas with abundant post-volcanic activities.

Previous mineralogical studies on cave sulfates precipitated in sulfidic-rich steam condensate alteration environments are known from many locations worldwide. Spallanzani (1797) provided the first written report describing alunogen $Al_2(SO_4)_3(H_2O)_{12}\cdot 5H_2O$, halotrichite $Fe^{2+}Al_2(SO_4)_4\cdot 22H_2O$, and an unidentified iron sulfate from the Alum Cave (Vulcano Island, Sicily). More recent accounts on the mineralogy of this unique volcanic cave highlights the presence of 22 sulfate minerals (Forti et al. 1996; Demartin et al. 2010). Rodgers et al. (2000) report a complex suite of minerals from another non-limestone cavity (Ruatapu Cave, New Zealand) developed in hydrothermally altered vitric tuffs. When acid sulfate weathering takes place in limestone caves, however, the mineralogy is dominated by gypsum. This is the case for the famous, presently active sulfidic-rich cave systems from Frasassi and Acquasanta (Italy; Galdenzi and Maruoka 2003; Galdenzi et al. 2010) and Villa Luz (Mexico; Hose et al. 2000). When the lithology exposed within carbonate caves varies, the sulfidic steam condensate mineralogy may be complex. Examples falling under this category include several caves from France, Romania, and Greece (Povară et al. 1972; Diaconu and Medeşan 1973; Audra and Hobléa 2007; Onac et al. 2009a; Lazaridis et al. 2011).

Rapidcreekite, ideally $Ca_2(SO_4)(CO_3)\cdot 4H_2O$, has only been found in nature at a very few localities; usually it is in association with gypsum and a carbonate mineral. The mineral was originally described by Roberts et al. (1986) from an iron-rich deposit in the Rapid Creek area of Yukon, Canada, then three years later by Walenta and Dunn (1989) from the Johann Mine (Black Forest, Germany) under a completely different setting (U-Co mineralization zone). In this later occurrence, rapidcreekite is associated primarily with camgasite, calcite, monohydrocalcite, and gypsum; iron containing minerals are absent there. Further localities are two mines in Norway and Germany, respectively, and a possible cave location in Czech Republic (Raade 1989;

* E-mail: bonac@usf.edu

Rüger et al. 1995; Žák et al. 2010). Synthetic rapidcreekite has also been identified as an intermediate phase during desalinization studies from solutions having a low carbonate to sulfate ratio (Dydo et al. 2003; Schausberger et al. 2009). Rapidcreekite was recently reported as the main hydration product in a ternary cement system where it formed via ettringite carbonation (Martínez-Ramírez and Fernández-Carrasco 2012).

Early in 2008, the mineral assemblages of several caves located along the Cerna Valley (SW Romania) and affected by ascending sulfide-rich thermo-mineral waters were investigated by Onac et al. (2009a), reporting the probable presence of rapidcreekite in the Diana Cave. The present paper describes this new occurrence of rapidcreekite in detail. Its discovery in the environment of the Diana Cave is significantly different from the other known localities mentioned above.

Location

Diana Cave settings

The Diana Cave is located in southwestern Romania in the old center of Băile Herculane, a famous thermal spa founded more than 2000 yr ago (Povară 2001). It opens on the right bank of the Cerna River at ~7 m above its thalweg and consists of a 22 m, V-shaped cave passage at the far end of which the Diana thermal spring emerges (Povară et al. 1972). The mean annual cave temperature is 22 °C, and relative humidity is 100% year around, except for the cold periods, when outside dry air enters the cave and causes a drop of the water vapor partial pressure (85–95%) and thus evaporative conditions prevail in the cave.

The regional geology is rather complex; its relationship with the karst of the Cerna Valley has been described in details elsewhere (Schmid et al. 1998; Povară et al. 2008; Wynn et al. 2010). Relevant to the current research is that the cave passage formed along the Diana Fault; this enables the contact between the Late Jurassic nodular limestone and the Early Cretaceous gray-black Iuta marls (Năstăseanu 1980).

Diana Cave Spring

As early as 1881, the thermal water (mean temperature ~51 °C; Povară et al. 2008) of Diana's Spring was confined (for balneotherapy purposes) within the cave by a dam built at its entrance. In the early 1970s, a narrow cave passage heading SE was enlarged to drain the thermal water outside in a retention basin, from where it is pumped in a series of thermal baths. During this work all cave passages were enlarged and the walls, especially where marl crops out, were reinforced using concrete. Consequently, the original cave morphology was altered and the mineral deposits that had precipitated over the cave walls (in form of efflorescences and crusts) were hidden behind the concrete wall. Since the construction, however, the acid sulfate corroded the concrete and the cave walls are now exposed on restricted areas allowing for sample collection.

Diana Cave hosts two thermal springs (referred as Diana 1 and 2, respectively; Povară et al. 2008). The total dissolved solids of the waters is around 5700 mg/L and contain on average 1392.5 mg/L Na^+, 725 mg/L Ca^{2+}, 3370 mg/L Cl^-, and abundant H_2S degasses into the cave atmosphere. The sodium-calcium-chloride type thermo-mineral water has a nearly neutral pH (~6.5), and its total sulfide and sulfate concentration is 37 and 92 mg/L, respectively (Marin 1984; Wynn et al. 2010). The Diana Springs show excess concentrations of methane in its thermal water (Cosma et al. 2008), which enables a nearly complete thermochemical sulfate reduction (TSR). This process generates high-$\delta^{34}S$ values (27.2 ‰) of SO_4^{2-} in the solution and high-dissolved sulfide concentrations (>37 mg/L as S^{2-}) with a $\delta^{34}S$ value that takes on the approximate isotopic signature of the total dissolved S (mean +17.4‰) (Wynn et al. 2010; Onac et al. 2011). From the spring hydrochemistry, temperature, regional hydrogeology, and sulfur isotopic signature, Povară et al. (2008) and Onac et al. (2011) concluded that the thermal waters around Băile Herculane Spa (including the Diana Springs) represent deeply circulating meteoric waters that are upwelling along stratigraphic boundaries or faults.

The milky color of the water flowing along the NW-SE passage results from suspended elemental sulfur and sub-millimeter thin gypsum rafts (not larger than 60 cm^2) precipitating at the water-air interface. The abundant sulfidic steam released by the hot waters emerging from the Diana Springs condenses on the colder bedrock surface. Subsequent oxidation/hydrolysis of sulfides creates sulfuric acid solutions (pH between 3 and 4.5), which react with the bedrocks to form a variety of sulfates and controls the resulting cave steam-heated (also called acid-sulfate) weathering environment of the Diana Cave.

The Diana Cave mineral association

The mineralogical investigations in the Diana Cave were carried out in two distinct periods. The first one occurred in the early 1970s when Povară et al. (1972) briefly reported on the presence of elemental sulfur, gypsum, and "halotrichite" in a general presentation of the caves affected by thermal waters in the lower section of the Cerna Valley. A year later, a detailed study of the acicular-prismatic crystals originally described as "halotrichite," proved to be in fact pickeringite (Diaconu and Medeşan 1973). The authors suggested that pickeringite precipitated from the reaction between the acidic thermal waters and the marls on the cave floor. In another study, Diaconu (1974) described the world's first cave occurrence of anhydrite from the same cave.

The mineralogical investigations revived in 2007 when the lead author received a 3 yr grant to study the sulfuric acid caves along the Cerna Valley. Due to its active sulfidic environment, the Diana Cave is a central point of research in the region. In two consecutive papers, Onac et al. (2009a, 2009b) confirmed the presence of halotrichite; in addition apjohnite, epsomite, tamarugite, as well as rapidcreekite were identified.

Neither tamarugite nor rapidcreekite were described from carbonate karst caves so far, thus prompting us for more elaborate studies; one is dedicated to tamarugite (Puscaş et al. 2013) and the present one to rapidcreekite.

Samples and methods

Nine samples of transparent to white or yellowish-brown efflorescences and damp aggregates were collected from exposed sections of the cave wall (middle and lower part) at the far end of the Diana Cave and from the upper part of the concrete piers that cover the man-made waterway, respectively. The patchy efflorescences in which rapidcreekite was later identified always form directly over the weathered limestone and are intimately associated with fibrous gypsum crystals. In the lowermost part of the walls and on the floor (within the same cave section)

directly overlying the weathered marls, halotrichite group minerals were found. The presence of rapidcreekite was documented in two of these nine samples.

Chemical analyses were performed using a JEOL 8900R Superprobe electron microprobe (EMPA) instrument at the Department of Earth Sciences, Florida International University. Analytical conditions were: 15 kV, 5 and 10 nA, defocussed electron-beam diameter of 30 µm (sample was moved to avoid decomposition of the mineral under the beam, WDX: peak count-time 60 s, background count-time 15 s). Apatite (Ca), anhydrite (SO_3), diopside2 (MgO), kaersutite2 (K_2O), and PlagAn65 (Na_2O, Al_2O_3) served as standards. The CO_2 and H_2O content in the samples was calculated by means of thermogravimetric method using a Netzsch thermal apparatus with the following working conditions: sample weight 1.5 g, heating rate 10°/min, and temperature range 20 to 1000 °C). Computation of the empirical formula was performed using MINCALC-V5 software (Bernhardt 2010).

The SEM investigations were carried out on a JEOL 6490 LV operated in low-vacuum mode and equipped with an EDS analytical system in the Lisa Muma Weitz Imaging Core Laboratories (University of South Florida).

Sulfur and oxygen isotopic composition of SO_4^{2-} in bulk sulfates and in rapidcreekite (hand picked under the microscope) was measured in the Stable Isotope Laboratory of the Department of Geology (USF) on a Delta V Isotope Ratio Mass Spectrometer (IRMS) using a Costech Elemental Analyzer and a Temperature Conversion Elemental Analyzer, respectively, coupled to the IRMS following the methods described in Nehring et al. (1977), Grassineau et al. (2001), and Wynn et al. (2010). The results were normalized to Cañon Diablo Troilite (CDT) and Vienna Standard Mean Ocean Water (VSMOW) using $\delta^{34}S$ and $\delta^{18}O$ values of the two International Atomic Energy Agency (IAEA) standards IAEA SO-5 ($\delta^{34}S = 0.5‰$; $\delta^{18}O = 12‰$) and IAEA SO-6 ($\delta^{34}S = -34.1‰$; $\delta^{18}O = -11‰$). The reproducibility between replicate standards in each run was estimated to be better than ±0.1 and ±0.3‰ (1σ), respectively. Geochemical equilibrium modeling and calculations of the saturation index of calcite (SI_{calc}) were completed using the geochemical speciation program PHREEQC (Parkhurst and Appelo 1999).

Results and discussion

Physical properties

Rapidcreekite appears either as transparent, euhedral to subhedral acicular crystals or, more commonly, in whitish clusters of flattened prismatic crystals with a silky lustre. Scanning-electron imaging of rapidcreekite reveals bundles of crystals flattened on {010} and elongated along [001] (Figs. 1a and 1b). A perfect cleavage is observed on {100}. Crystal length measurements range from 40 to 1500 µm ($\overline{X}$ = 321 µm, n = 107 individual crystals). Irregular and globular white mate aggregates were found growing upon the prismatic rapidcreekite crystals (Fig. 1b).

Chemical and isotopic composition

The average composition (in wt%) of rapidcreekite obtained from 7-point measurements on two crystals is: CaO 35.65; SO_3 24.97; Na_2O 0.291; MgO 0.173; Al_2O_3 0.07; CO_2 13.7; and H_2O 23.9 (total 98.75). The empirical formula based on 7 non-water O atoms pfu is $Ca_{1.98}Na_{0.029}Mg_{0.013}Al_{0.004}(S_{0.971}O_4)(C_{0.97}O_3)\cdot 4.13H_2O$, ideally, $Ca_2(SO_4)(CO_3)\cdot 4H_2O$. This composition is in accordance with the only analysis reported so far by Roberts et al. (1986) for the Yukon rapidcreekite.

Semi-quantitative EDS analyses taken at natural faces of the aggregates growing upon the rapidcreekite crystals show the presence of C, O, and Ca in an atomic ratio 1:1:1. This finding corresponds well with the observation from the experimental work of Dydo et al. (2003) and the crystallization experiment of precipitating synthetic analogues of gypsum and vaterite via rapidcreekite by Bots (2011). Both studies reported the formation of carbonates (mainly vaterite and aragonite) along with rapidcreekite.

The isotopic composition ($\delta^{34}S$ and $\delta^{18}O$) of rapidcreekite and bulk sulfate minerals occurring as crusts and efflorescences is listed in Table 1. The data set is homogeneous, showing ^{34}S-enriched $\delta^{34}S$ values (18 to 19.5‰ CDT) whereas the $\delta^{18}O$ values range from –9.7 to –7.8‰ VSMOW.

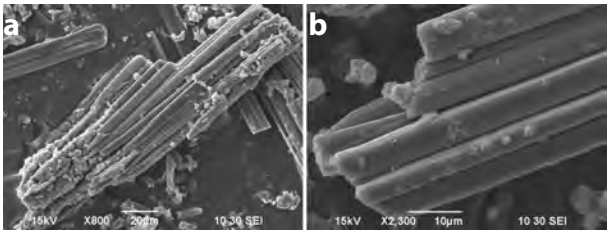

Figure 1. SEM image of bundle rapidcreekite crystals (**a**) and details showing the EDS-confirmed carbonate phase growing on their crystal surface (**b**).

X-ray experiments and refinement of the crystal structure

The crystal structure of rapidcreekite was determined by Cooper and Hawthorne (1996). However, the authors could not locate the H atoms during their final refinements and established the hydrogen-bond system based on crystal-chemical considerations. For a detailed discussion of the shape of the carbonate group, to verify the hydrogen bond scheme, and for a confident identification of rapidcreekite from a karst cave, a precision single-crystal study was performed at the University of Vienna (for details see Table 2). The crystal structure (Fig. 2) was refined starting from the atomic coordinates given by Cooper and Hawthorne (1996). The increased accuracy is mainly based on the larger number of observed reflections due to the use of an area detector, which allowed establishment of the location of the H atoms in a difference Fourier summation and the refinement of their atomic coordinates. However, the quality of the available crystals and the accuracy of the X-ray data allowed only an approximate location of the H atoms. Although there is no doubt on the main features of the hydrogen bond scheme, the actual positions of the H atoms' electrons are only approximate given the superposition of the H atom with inaccuracies in the electron density map. As a consequence, some O-H bonds differ from the expected values detected by X-ray investigations. The final structural parameters of rapidcreekite are given in Table 3; interatomic bond distances and the geometry of the hydrogen bonds in Table 4. A CIF[1,2] is available on deposit.

The results of the structural refinement compare well with the former description by Cooper and Hawthorne (1996). The atomic arrangement is characterized by rows of edge sharing $Ca1O_6(O_w)_2$ and $Ca2O_6(O_w)_2$ coordination polyhedra linked among each other by corners forming layers parallel to (100). Each of the SO_4 and CO_3 groups share edges with a $Ca1O_6(O_w)_2$ and a $Ca2O_6(O_w)_2$ coordination polyhedron. The layers are linked by hydrogen

[1] Deposit item AM-13-708, CIF. Deposit items are available two ways: For a paper copy contact the Business Office of the Mineralogical Society of America (see inside front cover of recent issue) for price information. For an electronic copy visit the MSA web site at http://www.minsocam.org, go to the *American Mineralogist* Contents, find the table of contents for the specific volume/issue wanted, and then click on the deposit link there.

[2] Further details of the crystal structure investigation may be obtained from Fachinformationszentrum Karlsruhe, 76344 Eggenstein-Leopoldshafen, Germany, on quoting the deposition number CSD-425547.

TABLE 1. $\delta^{34}S$ and $\delta^{18}O$ values for rapidcreekite and bulk sulfate minerals from Diana Cave, Romania

Sample no.	Mineral habit	$\delta^{34}S$ (‰)	$\delta^{18}O$ (‰)
	Rapidcreekite		
1770a	efflorescence	19.3	–8.7
1771a	efflorescence	18.0	–9.1
1773a	efflorescence	19.1	–9.3
1775	crust	19.5	–9.7
	Bulk sulfates		
1770b	efflorescence	19.4	–8.7
1771b	efflorescence	18.3	–9.1
1772	efflorescence	18.7	–9.1
1773b	efflorescence	19.2	–9.5
1776	crust	19.2	–7.8
1777	efflorescence	18.8	–9.4

TABLE 2. Summary of single-crystal X-ray data* and structure refinements of rapidcreekite

a (Å)	15.524(2)
b (Å)	19.218(3)
c (Å)	6.161(1)
Space group	*Pcnb*
V (Å^3)	1838.1(5)
Z	8
ρ_{calc} (g/cm^3)/μ (Mo*Kα*) (mm^{-1})	2.23/1.5
Range of data collection ($\pm h$ $\pm k$ $\pm l$) (°)	3 < 2θ < 65
Number of images/rotation angle per image (°)	1141/1
Scan mode (at 11 distinct ω-angles)	φ-scans
Scan time (s/°)/frame size (binned mode)	120/621×576 pixels
Detector-to-sample distance (mm)	40
Measured reflections	29694
Unique reflections (*n*)/reflections with $F_o > 4\sigma(F_o)$	3331/2592
$R_{int} = \Sigma\lvert F_o^2 - F_o^2(\text{mean})\rvert/\Sigma F_o^2$	0.058
$R1 = \Sigma(\lvert\lvert F_o\rvert - \lvert F_c\rvert\rvert)/\Sigma F_o$(3331/2592 reflections)	0.048/0.030
$wR2 = [\Sigma w(F_o^2 - F_c^2)^2/\Sigma\lvert wF_o^4\rvert]^{1/2}$	0.080
GooF = $\{\Sigma[w(F_o^2 - F_c^2)^2]/(n-p)\}^{0.5}$	1.059
Max Δ/σ; number of variable parameters (*p*)	<0.001; 162
Final difference Fourier map (e/Å^3)	–0.48 to +0.46

Note: $w = 1/\{\sigma^2(F_o^2) + [0.045\times P]^2 + 0.17\times P\}$; $P = ([\max(0,F_o^2)] + 2\times F_c^2)/3]$.
* NONIUS four-circle diffractometer equipped with a CCD detector and a 300 mm capillary-optics collimator (Mo tube, graphite monochromator). Unit-cell parameters were obtained by least-squares refinements of 2θ values. Data were corrected for background, Lorentz, polarization, and absorption effects (multi-scan method; complex scattering functions). Extinction was not observed. Programs used: COLLECT (Nonius 1999; Otwinowski and Minor 1997) and SHELXL-97 (Sheldrick 1997, 2008).

bonds only. The hydrogen bonds postulated by Cooper and Hawthorne (1996) for the water molecules O_w2H_2, O_w3H_2, and O_w4H_2 were confirmed. However, for both the hydrogen bonds of the O_w1H_2 molecule there is only one acceptor O atom. For one of the hydrogen bonds of the O_w4H_2 molecule the bifurcated hydrogen bond is confirmed. For the bifurcated H bond the bond angles O-H···O are 86 and 144°, whereas the others vary between 157 and 169°. Within the accuracy of the structure refinement, the H atom involved in the bifurcated hydrogen bond has a planar coordination by the donor atom and the two acceptor atoms [sum of bond angles 357(4)°].

The carbonate group features an approximately trigonal planar surrounding. The average C-O bond length of 1.284 Å corresponds exactly with the mean value of 1.284(18) Å reported by Zemann (1981) for 102 accurately determined carbonate groups of mineral structures. Despite the fact that the carbonate group shares two O-O edges with the CaO_8 polyhedra, the O-C-O bond angles deviate only slightly: they are 118.67(12) and 118.34(13)° for the shared and 122.95(14)° for the unshared edges. Noteworthy is the aplanarity of the carbonate group; the C atom lays 0.0157(16) Å above the plane defined

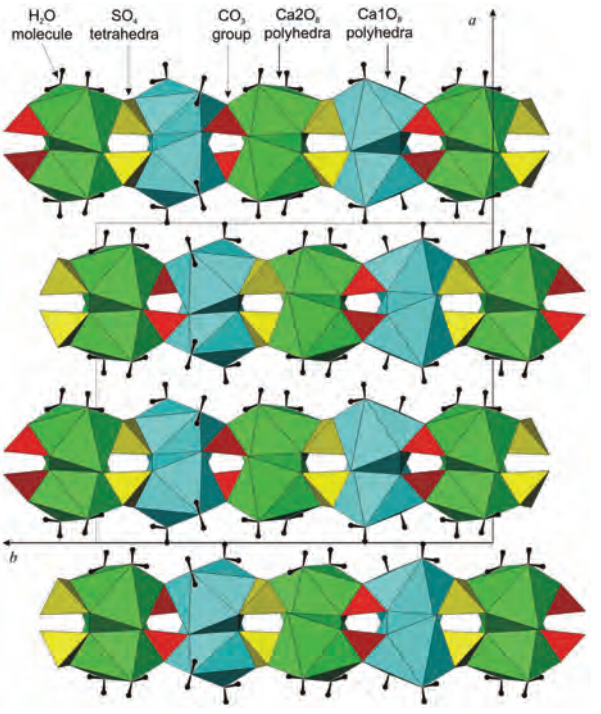

FIGURE 2. The crystal structure of rapidcreekite (program ATOMS; Dowty 1999). (Color online.)

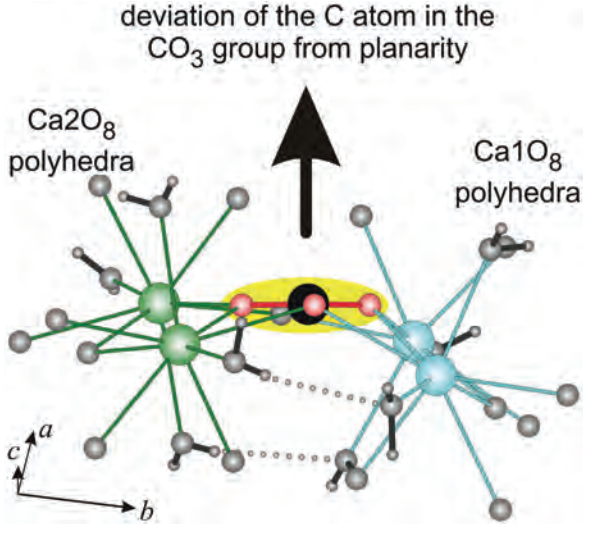

FIGURE 3. The surrounding of the carbonate group in rapidcreekite causing its aplanarity (program ATOMS; Dowty 1999). (Color online.)

by the three coordinating O atoms (Fig. 3). This deviation is caused by the electrostatic influence of the four Ca atoms in the surrounding of the carbonate group. Only one Ca2 atom is located slightly above the O-atom plane of the carbonate group [0.037(3) Å], whereas the further Ca2 and the two Ca1 atoms are significantly below this plane [0.687(2), 0.639(2), and 1.232(2) Å]. The deviation from planarity compares with those found in other carbonates like dolomite or bütschliite,

TABLE 3. Fractional atomic coordinates and displacement parameters of rapidcreekite

Atom	*x*	*y*	*z*	U_{equiv}/U_{iso}	U_{11}	U_{22}	U_{33}	U_{23}	U_{13}	U_{12o}
Ca1	0.334002(18)	0.289513(15)	0.20090(5)	0.01712(8)	0.01787(14)	0.01618(14)	0.01733(14)	–0.00086(10)	–0.00016(10)	–0.00035(10)
Ca2	0.327543(18)	0.053335(15)	0.18898(5)	0.01655(8)	0.01821(14)	0.01593(14)	0.01552(14)	0.00084(10)	0.00018(10)	0.00052(10)
S	0.16871(2)	0.419309(18)	0.02690(6)	0.01621(9)	0.01788(16)	0.01490(16)	0.01584(16)	–0.00090(12)	0.00004(12)	–0.00009(11)
C	0.19103(10)	0.17345(7)	0.4337(2)	0.0165(3)	0.0175(6)	0.0180(6)	0.0140(6)	0.0000(5)	–0.0007(5)	–0.0001(5)
O1	0.22452(7)	0.35836(6)	0.04875(19)	0.0250(2)	0.0278(5)	0.0202(5)	0.0268(6)	0.0006(4)	–0.0030(4)	0.0069(4)
O2	0.21343(7)	0.23291(5)	0.35720(18)	0.0204(2)	0.0235(5)	0.0166(5)	0.0212(5)	0.0020(4)	0.0030(4)	–0.0019(4)
O3	0.38966(7)	0.40374(6)	0.34196(18)	0.0239(2)	0.0254(5)	0.0229(5)	0.0235(6)	–0.0039(4)	0.0063(4)	–0.0011(4)
O4	0.37085(7)	0.17133(5)	0.07484(18)	0.0191(2)	0.0193(5)	0.0193(5)	0.0187(5)	0.0004(4)	–0.0034(4)	–0.0009(4)
O5	0.22870(7)	0.11704(5)	0.38274(18)	0.0243(2)	0.0299(6)	0.0191(5)	0.0239(5)	0.0012(4)	0.0093(5)	0.0048(4)
O6	0.28117(7)	0.48285(5)	0.48411(18)	0.0228(2)	0.0255(5)	0.0186(5)	0.0243(6)	–0.0012(4)	–0.0050(4)	0.0045(4)
O7	0.11778(7)	0.43255(6)	0.22415(18)	0.0242(2)	0.0277(6)	0.0232(5)	0.0217(5)	–0.0031(4)	0.0070(4)	–0.0029(4)
W1	0.08933(8)	0.23878(7)	0.0107(2)	0.0274(3)	0.0269(6)	0.0318(6)	0.0235(6)	0.0007(5)	0.0000(5)	–0.0040(5)
W2	0.04803(8)	0.32244(7)	0.4660(2)	0.0296(3)	0.0243(6)	0.0308(7)	0.0336(7)	0.0061(5)	–0.0049(5)	0.0004(5)
W3	0.07520(8)	0.02078(7)	0.3958(2)	0.0252(2)	0.0247(6)	0.0274(6)	0.0236(6)	–0.0041(5)	–0.0004(5)	–0.0006(5)
W4	0.43354(9)	0.09068(8)	0.4675(2)	0.0288(3)	0.0250(6)	0.0334(7)	0.0280(6)	0.0030(5)	–0.0040(5)	–0.0018(5)
$H_{Ow1\text{-}Ow1}$	0.0414(16)	0.2390(16)	0.033(4)	0.045(4)*						
$H_{Ow1\text{-}O2}$	0.1182(16)	0.2440(14)	0.116(5)	0.045(4)*						
$H_{Ow2\text{-}O4}$	0.003(2)	0.3337(14)	0.485(6)	0.045(4)*						
$H_{Ow2\text{-}O7}$	0.0623(19)	0.3598(15)	0.402(5)	0.045(4)*						
$H_{Ow3\text{-}Ow3}$	0.0372(18)	0.0193(17)	0.427(5)	0.045(4)*						
$H_{Ow3\text{-}O3}$	0.0906(17)	–0.0138(14)	0.338(5)	0.045(4)*						
$H_{Ow4\text{-}O3}$	0.4914(19)	0.1012(15)	0.425(5)	0.045(4)*						
$H_{Ow4\text{-}Ow1/Ow3}$	0.437(2)	0.0917(17)	0.553(5)	0.045(4)*						

Note: Anisotropic displacement parameters: exp $[-2\pi^2 \Sigma_{i=1}^{3} \Sigma_{j=1}^{3} U_{ij} a_i^* a_j^* h_i h_j]$.
* Constrained during refinement.

TABLE 4A. Interatomic bond lengths (Å) and bond angles (°) for rapidcreekite

Ca1-O1	2.3491(11)	Ca2-O5	2.2975(11)
Ca1-O2	2.3695(11)	Ca2-O6^{v}	2.4124(11)
Ca1-O_W2^{iii}	2.4183(13)	Ca2-O5^{iii}	2.4126(11)
Ca1-O_W1^{iv}	2.4517(13)	Ca2-O_W3^{iii}	2.4360(13)
Ca1-O4	2.4675(10)	Ca2-O4	2.4676(10)
Ca1-O2^{iii}	2.4919(11)	Ca2-O_W4	2.4837(13)
Ca1-O3	2.5142(12)	Ca2-O7^{v}	2.5289(11)
Ca1-O1^{iv}	2.6775(12)	Ca2-O6^{viii}	2.5318(12)
S-O1	1.4631(11)	C-O5	1.2712(17)
S-O6^{iii}	1.4718(11)	C-O2	1.2839(17)
S-O7	1.4719(11)	C-O4^{iv}	1.2964(18)
S-O3^{iii}	1.4862(11)		

TABLE 4B. Hydrogen bonds

Donor	H atom	Acceptor	D-H	H···A	D···A	D-H···A	H···D···H	A···D···A	A···H···A
O_w1	$H_{Ow1\text{-}Ow1}$	O_w1^{i}	0.76(3)	2.08(3)	2.807(2)	162(3)			
O_w1	$H_{Ow1\text{-}O2}$	O2	0.80(3)	2.11(3)	2.878(2)	163(3)	113(3)	131.88(3)	
O_w2	$H_{Ow2\text{-}O4}$	O4^{vi}	0.74(3)	2.13(3)	2.834(2)	160(3)			
O_w2	$H_{Ow2\text{-}O7}$	O7	0.85(3)	1.98(3)	2.806(2)	166(3)	94(3)	117.94(5)	
O_w3	$H_{Ow3\text{-}Ow3}$	O_w3^{vii}	0.62(3)	2.20(3)	2.782(2)	157(4)			
O_w3	$H_{Ow3\text{-}O3}$	O3^{v}	0.79(3)	1.96(3)	2.739(2)	169(3)	113(3)	100.27(7)	
O_w4	$H_{Ow4\text{-}O3}$	O3^{ii}	0.96(3)	1.92(5)	2.854(2)	165(3)			
O_w4	$H_{Ow4\text{-}Ow1/Ow3}$	O_w1^{iv}	0.53(3)	2.87(3)	2.881(2)	86(4)	96.11(5)		
O_w4	$H_{Ow4\text{-}Ow1/Ow3}$	O_w3^{iv}	0.53(3)	2.52(3)	2.964(2)	144(4)	100(4)	107.61(5)	127(1)

Note: Symmetry code: not specified *x,y,z*; ^{i} –*x*,–*y*+½,*z*; ^{ii} –*x*+1,–*y*+½,*z*; ^{iii} –*x*+½,*y*,*z*–½; ^{iv} –*x*+½,*y*,*z*+½; ^{v} –*x*+½,*y*–½,–*z*+½; ^{vi} *x*–½,–*y*+½,*z*+½; ^{vii} –*x*,–*y*,–*z*+1; ^{viii} *x*,*y*–½,–*z*+1.

with 0.018(1) and 0.014(2), respectively (Effenberger et al. 1981; Effenberger and Langhof 1984). An extremely large aplanarity of the carbonate group was reported for thaumasite, $Ca_3Si(OH)_6(CO_3)(SO_4)\cdot 12H_2O$ (Edge and Taylor 1971; Zemann and Zobetz 1981; Effenberger et al. 1983; Jacobsen et al. 2003; Gatta et al. 2012).

The equivalent isotropic displacement parameters U_{equiv} of the Ca, S, and C atoms are 0.01621(9) to 0.01712(18) Å^2, those of the oxygen atoms belonging to the anion groups are slightly larger [0.0191(2) to 0.025(2) Å^2] but smaller as compared to those of the oxygen atoms belonging to the water molecules 0.0252(3) to 0.0296(3) Å^2. The ratios longest/shortest axes of the principal mean square atomic displacement of U_{ij} are small for the Ca, S, and C atoms (1.140 to 1.295) but significantly larger for the O atoms belonging to the anion groups (1.455 to 2.408). It is worth noting that despite we found the largest U_{equiv} values for oxygen atoms in the water molecules, their ratios longest/shortest axes are only 1.440 to 1.858.

Origin of rapidcreekite

The occurrence of rapidcreekite along with gypsum, tamarugite, and other Al-bearing sulfate efflorescences is a notable feature of the present surficial sulfuric acid weathering environment of the Diana Cave. The peculiar setting responsible for the formation of this mineral assemblage is controlled by: (1) the development of the cave along the Diana Fault, and (2) a H_2S-rich thermo-mineral water source within the cave. The first condition is crucial in that the downthrown footwall block of the fault contains marls, which provides the necessary ingredients to produce tamarugite and minerals of the halotrichite group

that are part of the rapidcreekite paragenesis. The second factor is responsible for adding to the geochemical system vast amounts of H_2S-charged thermal waters, in which the H_2S is oxidized to H_2SO_4.

$$H_2S+2O_2 \leftrightharpoons 2H^+ + SO_4^{2-} \quad (1)$$

In the case of the Diana Cave, this oxidation occurs in some of the most reducing conditions of the thermal waters of the Cerna Valley, such that the $\delta^{18}O$ values of oxygen in the sulfate ion is derived predominantly from the thermal waters, rather than from atmospheric O_2. Once oxidized, the sulfate ions as well as the abundant H^+ ions react with limestone, buffering the acidity of the thermal waters by production of bicarbonate ion. Ultimately this process may drive the solution to gypsum (or anhydrite) saturation according to

$$2H^+ + SO_4^{2-} + 2CaCO_3 + 2H_2O \rightarrow Ca^{2+} + 2HCO_3^- + CaSO_4 \cdot 2H_2O. \quad (2)$$

Work by Dydo et al. (2003) and Schausberger et al. (2009) elucidates the geochemical conditions conducive to rapidcreekite precipitation. These authors have studied the controls of this mixed bicarbonate-sulfate system on carbonate mineral saturation, including equilibrium precipitation of carbonates, sulfates, and mixed carbonate-sulfate minerals such as rapidcreekite. Because rapidcreekite is more soluble than calcite, its precipitation requires low-carbonate concentrations relative to sulfate [in experiments of Dydo et al. (2003), when $CO_3^{2-}/SO_4^{2-} = 4.5\times10^{-3}$]. Busenberg and Plummer (1985) described more quantitatively the apparent equilibrium constant of carbonate-sulfate co-precipitates as

$$Ca_xNa_{(x-1)}CO_{3(y)}SO_{4(1-y)} \leftrightharpoons xCa^{2+} + (1-x)Na^+ + yCO_3^{2-} + (1-y)SO_4^{2-} \quad (3)$$

$$\log K = \log K_{CaCO3} + 6.3[(1 - y)/2] + 0.087(1 - x)/2. \quad (4)$$

Thus, log K of rapidcreekite (x = 1, y = 0) is 1.575 higher than that of calcite. Equilibrium modeling of typical sample chemical compositions from Diana 1 and 2 (Constantin, unpublished data; Ponta, unpublished data) produces calcite saturation indexes ($SI_{calcite}$) of 0.93–2.25. Given the effect of high-sulfate ion activity typical of the Diana Cave, the modeled equilibrium saturation index for rapidcreekite shows that at times the waters are supersaturated with respect to this theoretical rapidcreekite equilibrium constant ($SI_{rapidcreekite}$ = 0.65 to 0.66). Supersaturated conditions occur when the modeled equilibrium CO_3^{2-}/SO_4^{2-} ratio is low (0.06–0.46). As the pH of the solutions rise above 6.4 during gypsum precipitation (reaction 2), the waters may then precipitate rapidcreekite in addition to a "Ca-carbonate" mineral

$$3Ca^{2+} + 2HCO_3^- + SO_4^{2-} + 3H_2O \rightarrow Ca_2(SO_4)(CO_3)\cdot 4H_2O + \text{“}CaCO_3\text{”}. \quad (5)$$

Thus, the controlling factors in the distribution of various types of minerals are the activity of ions available (both in the bedrock and steam-condensed solutions), pH, and the local physical conditions (temperature, relative humidity, cave ventilation). If this interpretation is correct, the narrow stability range of rapidcreekite explains the relatively few observations of the mineral in nature.

The "carbonate phase" formed in reaction 5 could be the one observed during the SEM-EDS scan as aggregates growing on rapidcreekite's crystal faces (Fig. 1b). Given the presence of epsomite ($MgSO_4\cdot 7H_2O$) in the mineral assemblage of the Diana Cave (in the same part of the cave where gypsum and rapidcreekite were identified), we tentatively conclude that the "carbonate mineral" might be aragonite or even vaterite as Mg^{2+} is known (from nature and laboratory experiments) to promote the growth of either minerals over calcite (Folk 1974; Reddy and Nancollas 1976; Carlson 1983; Kawano et al. 2009; Bots 2011).

Consequently, we conclude that rapidcreekite can form simultaneously or shortly after the full crystallization of gypsum and prior to the growth of the "$CaCO_3$ phase" when both SO_4^{2-} and CO_3^{2-} are present in the system. Due to the presence of limestone and gypsum, which both release Ca^{2+} when they dissolve, we suggest that the common-ion effect may initiate the precipitation of rapidcreekite and be responsible for the deposition of the carbonate phase. The Al sulfates precipitate only when the pH of the steam-condensed fluids drops below 4.5 and favorable ionic activities occur (Martin et al. 1999; Rodgers et al. 2000; Hall et al. 2003). However, it appears that the Al-bearing sulfates form ephemeral efflorescences that may dissolve during cold seasons when relative humidity in the cave atmosphere decreases as dry air enters from outside. An increase of rainwater percolating into the cave will have a similar effect. Both these factors impact the pH at which the sulfate acid reactions happen and thus control the stability and formation of tamarugite, epsomite, and rapidcreekite. Regeneration follows dissolution, once appropriate conditions are restored within the cave.

The $\delta^{34}S$ values of the sulfate samples from the Diana Cave indicate an almost complete, sulfate-limited TSR (high H_2S/SO_4^{2-}) under highly anoxic conditions in the deep thermal water. Such values are consistent with an oxidation of dissolved sulfide in springs of the lower Cerna Valley described by Wynn et al. (2010). This suggests that S in the investigated sulfate minerals is derived from dissolution of primary sulfates from marine limestone followed by reduction in the thermal aquifer and then by re-oxidation in the cave (both in the hot water and atmosphere). The $\delta^{18}O$ values of the sulfate minerals indicate an abundant ^{18}O exchange with $H_2O_{(l)}$ during hydration and near complete exclusion of oxygen derived from $O_{2(aq)}$ in sulfate minerals from the Diana Cave (Onac et al. 2011).

The results presented in this study provide further evidence that rapidcreekite precipitates, and is a persistent mineral phase in the sulfide-rich steam condensate environment of Diana Cave if optimal pH, temperature, ion activity, and relative humidity conditions are met. These conditions, however, are essentially different from other terrestrial records previously documented. Because rapidcreekite was reported from a handful of locations, all different with regard to their geological and physico-chemical parameters, additional information is required before its thermodynamic stability field (for both low or high temperatures) is revealed.

ACKNOWLEDGMENTS

The Domogled-Valea Cernei National Park granted approval to collect samples for analysis. C. Marin from the Emil Racoviță Institute of Speleology and G. Ponta (PELA) offered many insights into Cerna Valley hydrochemistry; Vera Dârmiceanu, Lucian Nicoliță, and Daniel Vereș assisted us during the field campaigns. The authors greatly appreciate the constructive reviews and suggestions from Joel Grice, an anonymous referee, Ron Peterson (Technical Editor), as well as the Associate Editor, Diego Gatta. Type material is deposited in the Mineralogical Museum of the Babes-Bolyai University in Cluj Napoca, Romania. This work has received financial support from the Romanian National Authority for Scientific Research (Grant IDEI_544 to B.P.O.). We dedicate this paper to Josef Zemann on the occasion of his 90th birthday anniversary.

REFERENCES CITED

Audra, P. and Hobléa, F. (2007) The first cave occurrence of jurbanite [Al(OH SO_4)·$5H_2O$], associated with alunogen [$Al_2(SO_4)_3$·$17H_2O$] and tschermigite [$NH_4Al(SO_4)_2$·$12H_2O$]: Thermal-sulfidic Serpents Cave, France. Journal of Cave and Karst Studies, 69, 243–249.

Bernhardt, H.-J. (2010) MINCALC-V5, a non EXCEL based computer program for general electron-microprobe mineral analyses data processing. IMA 2010, 20th International Mineralogical Association Congress, Budapest. Acta Mineralogica Petrographica Abstract Series, 6, 869.

Bots, P. (2011) Experimental investigations of calcium carbonate mineralogy in past and future oceans, 194 p. Ph.D. thesis, The University of Leeds, U.K.

Busenberg, E. and Plummer, N.L. (1985) Kinetic and thermodynamic factors controlling the distribution of SO_4^{2-} and Na^+ in calcites and selected aragonites. Geochimica et Cosmochimica Acta, 49, 713–725.

Carlson, W.D. (1983) The polymorphs of $CaCO_3$ and the aragonite-calcite transformation. In R.J. Reeder, Ed., Carbonates: Mineralogy and chemistry, 11, p. 191–225, Reviews in Mineralogy, Mineralogical Society of America, Chantilly, Virginia.

Cooper, M.A. and Hawthorne, F.C. (1996) The crystal structure of rapidcreekite, $Ca_2(SO_4)(CO_3)(H_2O)_4$, and its relation to the structure of gypsum. Canadian Mineralogist, 34, 99–106.

Cosma, C., Suciu, I., Jäntschi, L., and Bolboacă, S.D. (2008) Ion-molecule reactions and chemical composition of emanated from Herculane Spa geothermal sources. International Journal of Molecular Sciences, 9, 1024–1033.

Demartin, F., Castellano, C., Gramaccioli, C.M., and Campostrini, I. (2010) Aluminocoquimbite, $AlFe(SO_4)_3$·$9H_2O$, a new aluminum iron sulphate from Grotta Dell'Allume, Vulcano, Aeolian Islands, Italy. Canadian Mineralogist, 48, 1465–1468.

Diaconu, G. (1974) Quelques considérations sur la présence de l'anhydrite dans la grotte "Pestera Diana" (Băile Herculane-Roumanie). Travaux Institute Spéologie "Emile Racovitza", 13, 191–194.

Diaconu, G. and Medeşan, A. (1973) Sur la présence de pickeringite dans la grotte Diana (Băile Herculane, Roumanie). Travaux Institute Spéologie "Emile Racovitza," 12, 303–309.

Dowty, E. (1999) ATOMS 5.0, a computer program. Kingsport, Tennessee.

Dydo, P., Turek, M., and Ciba, J. (2003) Scaling analysis of nanofiltration systems fed with saturated calcium sulfate solutions in the presence of carbonate ions. Desalination, 159, 245–251.

Edge, R.A. and Taylor, F.W. (1971) Crystal structure of thaumasite, [$Ca_3Si(OH)_6$·$12H_2O$][SO_4][CO_3]. Acta Crystallographica, B27, 594–601.

Effenberger, H. and Langhof, H. (1984) On the planarity of the CO_3 group in buetschliite, dipotassium calcium dicarbonate, $K_2Ca(CO_3)_2$. Acta Crystallographica, C40, 1299–1300.

Effenberger, H., Mereiter, K., and Zemann, J. (1981) Crystal structure refinements of magnesite, calcite, rhodochrosite, siderite, smithonite, and dolomite, with discussion of some aspects of the stereochemistry of calcite type carbonates. Zeitschrift für Kristallographie, 156, 233–243.

Effenberger, H., Kirfel, A., Will, G., and Zobetz, E. (1983) A further refinement of the crystal structure of thaumasite, $Ca_3Si(OH)_6CO_3SO_4$·$12H_2O$. Neues Jahrbuch für Mineralogie Monatshefte, 60–68.

Folk, R.L. (1974) The natural history of crystalline calcium carbonate: effect of magnesium content and salinity. Journal of Sedimentary Petrology, 44, 40–53.

Forti, P., Panzica La Manna, M., and Rossi, A. (1996) The peculiar mineralogical site of the Alum cave (Vulcano, Sicily). In P. Oromí, Ed., 7th International Symposium on Vulcanospeleology, Santa Cruz de La Palma, Canary Islands, November 1994, p. 35–44, Amelia Romero, Barcelona.

Galdenzi, S. and Maruoka, T. (2003) Gypsum deposits in the Frasassi Caves, Central Italy. Journal of Cave and Karst Studies, 65, 111–125.

Galdenzi, S., Cocchioni, F., Filipponi, G., Morichetti, L., Scuri, S., Selvaggio, R., and Cocchioni, M. (2010) The sulfidic thermal caves of Acquasanta Terme (central Italy). Journal of Cave and Karst Studies, 72, 43–58.

Gatta, G.D., McIntyre, G.J., Swanson, J.G., and Jacobsen, S.D. (2012) Minerals in cement chemistry: A single-crystal neutron diffraction and Raman spectroscopic study of thaumasite, $Ca_3Si(OH)_6(CO_3)(SO_4)$·$12H_2O$. American Mineralogist, 97, 1060–1069.

Grassineau, N., Mattey, D., and Lowry, D. (2001) Sulfur isotope analysis of sulfide and sulfate minerals by continuous low-isotope ratio mass spectrometry. Analytical Chemistry, 73, 220–225.

Hall, A.J., Fallick, A.E., Perdikatsis, V., and Photos-Jones, E. (2003) A model for the origin of Al-rich efflorescences near fumaroles, Melos, Greece: Enhanced weathering in a geothermal setting. Mineralogical Magazine, 67, 363–379.

Hill, C.A. and Forti, P. (1997) Cave Minerals of the World, 2nd ed., 463 p. National Speleological Society, Huntsville, Alabama.

Hose, L.D., Palmer, A.N., Palmer, M.V., Northup, D.E., Boston, P.J., and DuChene, H.R. (2000) Microbiology and geochemistry in a hydrogen-sulphide-rich karst environment. Chemical Geology, 169, 399–423.

Jacobsen, S.D., Smyth, J.R., and Swope, R.J. (2003) Thermal expansion of hydrated six-coordinate silicon in thaumasite, $Ca_3Si(OH)_6CO_3SO_4$·$12H_2O$. Physics and Chemistry of Minerals, 30, 321–329.

Kawano, J., Shimobayashi, N., Miyake, A., and Kitamura, M. (2009) Precipitation diagram of calcium carbonate polymorphs: Its construction and significance. Journal of Physics: Condensed Matter, 21, 425102.

Lazaridis, G., Melfos, V., and Papadopoulou, L. (2011) The first cave occurrence of orpiment (As_2S_3) from the sulphuric acid caves of Aghia Paraskevi (Kassandra Peninsula, N. Greece). International Journal of Speleology, 40, 133–139.

Marin, C. (1984) Hydrochemical considerations in the lower Cerna river basin. Theoretical and Applied Karstology, 1, 173–182.

Martin, R., Rodgers, K.A., and Browne, P.R.L. (1999) The nature and significance of sulphate-rich, aluminous efflorescences from the Te Kopia geothermal field, Taupo Volcanic Zone, New Zealand. Mineralogical Magazine, 63, 413–419.

Martínez-Ramírez, S. and Fernández-Carrasco, L. (2012) Carbonation of ternary cement systems. Construction and Building Materials, 27, 313–318.

Năstăseanu, S.V. (1980) Géologie des Monts Cerna. Anuarul Institutului de Geologie şi Geofizică, LIV, 153–280.

Nehring, N.L., Bowen, P.A., and Truesdell, A.H. (1977) Technique for the conversion to carbon dioxide of oxygen from dissolved sulfate in thermal waters. Geothermics, 5, 63–66.

Nonius, B.V. (1999) "Collect." Data collection software. Bruker AXS, Karlsruhe, Germany.

Onac, B.P. (2012) Minerals. In W.B. White and D.C. Culver, Eds., Encyclopedia of Caves, p. 499–508. Academic Press, Chennai.

Onac, B.P. and Forti, P. (2011a) Minerogenetic mechanisms occurring in the cave environment: an overview. International Journal of Speleology, 40, 79–98.

——— (2011b) State of the art and challenges in cave minerals studies. Studia UBB Geologia, 56, 33–42.

Onac, B.P., Sumrall, J., Tămaş, T., Cizmaş, C., Dârmiceanu, V., Povară, I., and Nicolită, L. (2009a) Mineralogical and stable isotope investigations of minerals from caves on Cerna Valley (Romania). In W.B. White, Ed., Proceedings of the 15th International Congress of Speleology, 1, p. 318–323. Kerrville, Texas.

Onac, B.P., Sumrall, J., Tămaş, T., Povară, I., Kearns, J., Dârmiceanu, V., Vereş, D., and Lascu, C. (2009b) The relationship between cave minerals and hypogene activity along the Cerna Valley (SW Romania). Acta Carsologica, 38, 67–79.

Onac, B.P., Wynn, J.G., and Sumrall, J.B. (2011) Tracing the sources of cave sulfates: A unique case from Cerna Valley, Romania. Chemical Geology, 288, 105–114.

Otwinowski, Z. and Minor, W. (1997) Processing of X-ray diffraction data collected in oscillation mode. In C.W.J. Carter and R.M. Sweet, Eds., Methods in Enzymology, 276, p. 307–326. Academic Press, San Diego, California.

Parkhurst D.L. and Appelo C.A.J. (1999) User's guide to PHREEQC (Version 2)—a computer program for speciation, batch-reaction, one-dimensional transport, and inverse geochemical calculations. U.S. Geological Survey Water Resources Investigations Report 99-4259, 312 p.

Povară, I. (2001) Thermal springs in Băile Herculane (Romania). In P.E. LaMoreaux and J.T. Tanner, Eds., Spring and Bottled Waters of the World: Ancient history, source, occurrence, quality, and use, p. 210–216. Springer, Berlin.

Povară, I., Diaconu, G., and Goran, C. (1972) Observations préliminaires sur les grottes influencées par les eaux thermo-minérales de la zone Băile-Herculane. Travaux Institute Spéologie "Emile Racovitza," 11, 355–365.

Povară, I, Simion, G., and Marin, C. (2008) Thermo-mineral waters from the Cerna Valley Basin (Romania). Studia UBB Geologia, 53, 41–54.

Puscaş, C.M., Onac, B.P., Effenberger, H.S., and Povară, I. (2013) Tamarugite-bearing paragenesis formed by sulphate acid alteration in Diana Cave, Romania. European Journal of Mineralogy, 25, in press, DOI: 10.1127/0935-1221/2013/0025-2294.

Raade, G. (1989) Etter Neumann Svovel. Norske Amatørgeologers Sammenslutning-nytt, 16, 49.

Reddy, M.M. and Nancollas, G.H. (1976) The crystallisation of calcium carbonate: IV. The effect of magnesium, strontium, and sulfate ions. Journal of Crystal Growth, 35, 33–38.

Roberts, A.C., Ansell, H.G., Jonasson, I.R., Grice, J.D., and Ramik, R.A. (1986) Rapidcreekite, a new hydrated calcium sulfate-carbonate from the Rapid Creek area, Yukon Territory. Canadian Mineralogist, 24, 51–54.

Rodgers, K.A., Hamlin, K.A., Browne, P.R.L., Campbell, K.A., and Martin, R. (2000) The steam condensate alteration mineralogy of Ruatapu cave, Orakei

Korako geothermal field, Taupo Volcanic Zone, New Zealand. Mineralogical Magazine, 64, 125–142.
Rüger, F., Senf, L., and Witzke, T. (1995) Die Saalfelder Feengrotten: Seltene Sekundärmineralien aus Thüringen. Lapis, 20, 15–26.
Schausberger, P., Mustafa, G.M., Leslie, G., and Friedl, A. (2009) Scaling prediction based on thermodynamic equilibrium calculation—scopes and limitations. Desalination, 244, 31–47.
Schmid, S.M., Berza, T., Diaconescu, V., Froitzheim, N., and Fügenschuh, B. (1998) Orogen-parallel extension in the Southern Carpathians. Tectonophysics, 297, 209–228.
Sheldrick, G.M. (1997) SHELXL-97, a program for crystal structure refinement. University of Göttingen, Germany.
——— (2008) A short history of SHELX. Acta Crystallographica, A64, 112–122.
Spallanzani, L. (1797) Viaggi alle Due Sicilie ed in alcune parti dell'Appennino, 2, 202–206.
Walenta, K. and Dunn, P.J. (1989) Camgasit, ein neues Calcium-Magnesiumarsenatmineral der Zusammensetzung $CaMg(AsO_4)(OH)\cdot 5H_2O$ von Wittichen im mittleren Schwarwald. Aufschluss, 40, 369–372.
Wynn, J.G., Sumrall, J.G., and Onac, B.P. (2010) Sulfur isotopic composition and the source of dissolved sulfur species in thermo-mineral springs of the Cerna Valley, Romania. Chemical Geology, 271, 31–43.
Žák K., Skála R., Filippi M., and Plášil J. (2010) Ikaite—little known mineral of iced caves: occurence in seasonal cave ice formations of the Koda Cave (Bohemian Karst). Bulletin mineralogicko-petrologického oddělení Národního muzea v Praze, 18, 109–115 (in Czech).
Zemann, J. (1981) Zur Strukturchemie der Karbonate. Fortschritte der Mineralogie, 89, 95–116.
Zemann, J. and Zobetz, E. (1981) Do the carbonate groups in thaumasite have anomalously large deviations from coplanarity? Kristallografija, 26, 1215–1217.

Manuscript received December 24, 2012
Manuscript accepted March 8, 2013
Manuscript handled by G. Diego Gatta